Maize Tricin-Oligolignol Metabolites and Their Implications for Monocot Lignification[1][OPEN]

Wu Lan[2], Kris Morreel[2], Fachuang Lu, Jorge Rencoret, José Carlos del Río, Wannes Voorend, Wilfred Vermerris, Wout Boerjan*, and John Ralph*

Department of Energy Great Lakes Bioenergy Research Center, Wisconsin Energy Institute (W.L., F.L., J.Ra.), Department of Biological System Engineering (W.L., J.Ra.), and Department of Biochemistry (F.L., J.Ra.), University of Wisconsin, Madison, Wisconsin 53726; Department of Plant Systems Biology, Vlaams Instituut voor Biotechnologie, B–9052 Ghent, Belgium (K.M., W.Vo., W.B.); Department of Plant Biotechnology and Bioinformatics, Ghent University, B–9052 Ghent, Belgium (K.M., W.Vo., W.B.); State Key Laboratory of Pulp and Paper Engineering, South China University of Technology, 510641 Guangzhou, People's Republic of China (F.L.); Instituto de Recursos Naturales y Agrobiologia de Sevilla, Consejo Superior de Investigaciones Científicas, 41012 Seville, Spain (J.Re., J.C.d.R.); and Department of Microbiology and Cell Science, Institute of Food and Agricultural Sciences (IFAS), and Genetics Institute, University of Florida, Gainesville, Florida 32611 (W.Ve.)

ORCID IDs: 0000-0002-0677-3085 (W.L.); 0000-0002-3121-9705 (K.M.); 0000-0003-2728-7331 (J.Re.); 0000-0002-3040-6787 (J.C.d.R.); 0000-0001-9254-1557 (W.Vo.); 0000-0002-4582-3436 (W.Ve.); 0000-0003-1495-510X (W.B.); 0000-0002-6093-4521 (J.Ra.).

Lignin is an abundant aromatic plant cell wall polymer consisting of phenylpropanoid units in which the aromatic rings display various degrees of methoxylation. Tricin [5,7-dihydroxy-2-(4-hydroxy-3,5-dimethoxyphenyl)-4H-chromen-4-one], a flavone, was recently established as a true monomer in grass lignins. To elucidate the incorporation pathways of tricin into grass lignin, the metabolites of maize (*Zea mays*) were extracted from lignifying tissues and profiled using the recently developed 'candidate substrate product pair' algorithm applied to ultra-high-performance liquid chromatography and Fourier transform-ion cyclotron resonance-mass spectrometry. Twelve tricin-containing products (each with up to eight isomers), including those derived from the various monolignol acetate and *p*-coumarate conjugates, were observed and authenticated by comparisons with a set of synthetic tricin-oligolignol dimeric and trimeric compounds. The identification of such compounds helps establish that tricin is an important monomer in the lignification of monocots, acting as a nucleation site for starting lignin chains. The array of tricin-containing products provides further evidence for the combinatorial coupling model of general lignification and supports evolving paradigms for the unique nature of lignification in monocots.

Lignin is one of the major components in plant cell walls and is deposited predominantly in the walls of secondarily thickened cells. It is a complex phenylpropanoid polymer composed primarily of *p*-hydroxyphenyl (H), guaiacyl (G), and syringyl (S) units derived from the monolignols *p*-coumaryl **2H**, coniferyl **2G**, and sinapyl **2s** alcohols, respectively (Fig. 1; Freudenberg and Neish, 1968). These monolignols are biosynthesized in the cytoplasm and translocated to the cell wall, where they are oxidized by laccases and peroxidases to monolignol radicals (Boerjan et al., 2003; Dixon and Reddy, 2003; Ralph et al., 2004b; Vanholme et al., 2008, 2010; Bonawitz and Chapple, 2010; Mottiar et al., 2016). The polymer can be started by radical coupling between two monolignol radicals to form a dehydrodimer from which the chain extends by endwise polymerization with additional monolignols, producing β-O-4-, β-5-, β-1-, and β-β-linked units in the lignin. Two growing oligomers also may radically couple to increase the polymer size, producing 4-O-5- and 5-5-linked units. During such radical coupling reactions, therefore, the monomer-derived units are linked together via various C-C and C-O bonds with

different frequencies depending primarily on the monomer distribution and supply (Ralph et al., 2004b).

A rather remarkable discovery regarding monocot lignins was made recently during a characterization study in wheat (*Triticum aestivum*; del Río et al., 2012b). Previously unassigned correlation peaks in short-range two-dimensional ^{1}H-^{13}C correlation (heteronuclear single-quantum coherence, HSQC) NMR spectra of wheat (and other monocot) lignins were ultimately attributed to tricin **1** (Fig. 1), a flavone, that was shown by long-range correlation (heteronuclear multiple-bond correlation, HMBC) experiments to be etherified by putative 4'-O-β-coupling with coniferyl alcohol **2G**. Although tricin itself, various glycosides, and the flavonolignan tricin 4'-O-(β-guaiacylglyceryl) ether **3G** are known (Bouaziz et al., 2002), as reviewed recently (Li et al., 2016), more profound implications arose from the demonstrated presence of this structure in polymeric lignins (del Río et al., 2012a, 2012b, 2015; Rencoret et al., 2013), as recently fully established by biomimetic coupling reactions and product authentication (Lan et al., 2015). This was the first time a phenolic derived from a pathway independent of the canonical monolignol

biosynthetic pathway was shown to polymerize into lignin in wild-type plants. Second, tricin's structure, and its inability to undergo radical dehydrodimerization (below), implies that it can only start a lignin chain and cannot be incorporated into an existing one. Tricin, therefore, provides a nucleation site for lignin chain growth in a manner analogous to that proposed for arabinoxylan-bound ferulates (Ralph et al., 1995, 2004a, 2004b; Ralph, 2010). (We prefer not to use the term initiation site, as this implies some kind of active role [Ralph, 2010]). Given the facile detection of tricin in monocot lignins analyzed to date, a modest fraction of lignin chains must be covalently linked with tricin (at their starting ends).

We recently supported the involvement of tricin in lignification in the first of these reports (del Río et al., 2012b) by synthesizing a variety of authentic compounds **3** to confirm the veracity of the NMR assignments and have shown that tricin indeed cross couples with all three monolignols **2** via the radical coupling reactions that typify lignification (Lan et al., 2015). Tricin was shown to not undergo dehydrodimerization, which meant that it is restricted to cross-coupling reactions (with monolignols) during lignification, and was found even in the highest M_r fractions of the lignin isolated from maize (*Zea mays*; Lan et al., 2015).

In this study, we aimed to elucidate the incorporation pathways of tricin into maize lignins by applying liquid chromatography-mass spectrometry (LC-MS)-based

tools developed for oligolignol profiling (Morreel et al., 2004a, 2004b, 2006, 2010a, 2010b, 2014). We sought to provide evidence that tricin undergoes coupling with monolignols **2** and that endwise chain extension polymerization continues in planta. What was not fully anticipated was the array of tricin-oligolignols derived not only from tricin's coupling with monolignols but also with acylated monolignols (both acetates and *p*-coumarates) known to be involved in maize lignification (Ralph, 2010). The variety of structures extracted from maize and implicated by mass spectrometric analysis, and then in many cases authenticated via the synthesis of genuine compounds, is not only evidence for tricin's role in lignification but additionally provides compelling support for the combinatorial nature of the lignification process itself.

RESULTS

Metabolite Profiling by Candidate Substrate Product Pair Analysis

The phenolics from the (lignifying) internode bearing the maize cob were extracted with methanol and profiled via ultra-HPLC coupled to Fourier transform-ion cyclotron resonance-mass spectrometry (Morreel et al., 2004a, 2004b, 2014; Niculaes et al., 2014; Dima et al., 2015) to reveal the presence of tricin-oligolignols. Using the recently developed candidate substrate product pair (CSPP) algorithm (Morreel et al., 2014), a network was constructed in which mass-to-charge ratio (*m/z*) features that might be derived from each other via well-known enzymatic or chemical conversions are connected. This approach facilitates the tracking of *m/z* features representing similar compounds. Subsequently, network nodes of the tricin-oligolignol subnetwork were further characterized via tandem mass spectrometry, i.e. MS^n-based oligolignol sequencing (Morreel et al., 2010a, 2010b). This approach revealed a rather expansive set of tricin-oligolignol compounds **3**, **4**, and **5** (Fig. 1). The compounds include the products of coupling of all three monolignols **2** (at their usual β positions) with tricin **1** (at its 4′-*O* position), resulting in the tricin-4′-*O*-(β-arylglyceryl) or arylglycerol-β-*O*-4′-tricin ethers **3**, along with the products **3G′/S′** and **3G″/S″** from the coupling of tricin with the acylated monolignols, the coniferyl and sinapyl acetates, and the *p*-coumarate conjugates **2′** and **2″** (Fig. 1; Table I). Even more striking was the suggested presence of the trimers **4** and **5** resulting from the tricin-(4′-*O*-β)-monolignol with a further 4-*O*-β or 5-β linkage to another (acylated) monolignol (Fig. 1; Table I). All of the observed compounds, along with their retention times, *m/z* values, and formulae, are listed in Table I.

Syntheses of Authentic Compounds

Over the past few years, an understanding of the gas-phase fragmentation patterns that results when oligolignol anions are subjected to collision-induced

Figure 1. Tricin **1** and its oxidative coupling with monolignols **2** and monolignol conjugates **2'** and **2''** to produce tricin-oligolignols **3** (dimers), **4** (trimers), and **5** (trimers). Primes are used to indicate the acylation of monolignols and derived units in the polymer, and small uppercase letters H, G, and S are used to designate the *p*-hydroxyphenyl, guaiacyl, and syringyl nature of the aromatic rings (and therefore the moiety's derivation from its monolignol, *p*-coumaryl, coniferyl, or sinapyl alcohol); we also refer to the A and B rings, as shown, in trimers **4**. For example, the hypothetical compound formed by the coupling of coniferyl acetate **2G'** with tricin, followed by further chain extension by coupling the product dimer with sinapyl *p*-coumarate **2s''**, would be designated as **4G's''**; in various tables, we also designate this with the more descriptive shorthand T-(4-*O*-β)-G'-(4-*O*-β)-S'', which indicates the coupling modes from the starting tricin to the final sinapyl *p*-coumarate, in this case. The two structures designated with asterisks are synthesized authentic compounds that were not found among the maize metabolites.

dissociation (CID) has allowed us to become more confident with the structural assignments of the peaks revealed by LC-MS. Nevertheless, it is crucial to rigorously identify any new classes of compounds, such as the tricin-oligolignols and their variously acylated counterparts implicated here, by absolute authentication via their independent chemical synthesis. We have accomplished that via the synthesis of eight authentic compounds (Fig. 1): seven 4'-O-β cross-coupled dimers **3H**, **3G**, **3s**, **3G'**, **3s'**, **3G''**, and **3s''** and the trimer **4sG**. The fragmentation patterns of these compounds then provided sufficient support to confidently characterize analogous

Table I. *Tricin-oligolignols detected in maize*

No.	t_R	m/z	Formula	Δppm	Shorthand Name	Elucidation Level[a]
Dimers						
3H	19.9	495.12891	$C_{26}H_{23}O_{10}$	−1.5	T-(4-O-βt)-H	Identified
3H	20.6	495.12907	$C_{26}H_{23}O_{10}$	−1.2	T-(4-O-βe)-H	Identified
3G	20.4	525.13906	$C_{27}H_{25}O_{11}$	−2.2	T-(4-O-βt)-G	Identified
3G	21.2	525.13889	$C_{27}H_{25}O_{11}$	−2.6	T-(4-O-βe)-G	Identified
3G'	24.7	567.14943	$C_{29}H_{27}O_{12}$	−2.4	T-(4-O-βt)-G'	Identified
3G'	25.0	567.15031	$C_{29}H_{27}O_{12}$	−0.8	T-(4-O-βe)-G'	Identified
3G''	25.7	671.17480	$C_{36}H_{31}O_{13}$	−3.3	T-(4-O-βt)-G''	Identified
3G''	25.9	671.17447	$C_{36}H_{31}O_{13}$	−3.8	T-(4-O-βe)-G''	Identified
3s''	25.5	701.18628	$C_{37}H_{33}O_{14}$	−1.9	T-(4-O-βt)-S''	Identified
3s''	25.7	701.18532	$C_{37}H_{33}O_{14}$	−3.2	T-(4-O-βe)-S''	Identified
3G^{αOMe}	24.7	539.15522	$C_{28}H_{27}O_{11}$	−1.2	T-(4-O-β)-G^{αOMe}	Annotated
Trimers						
4GG	18.9	721.21084	$C_{37}H_{37}O_{15}$	−4.1	T-(4-O-β)-G-(4-O-β)-G	Annotated
4GG	19.2	721.21151	$C_{37}H_{37}O_{15}$	−3.2	T-(4-O-β)-G-(4-O-β)-G	Annotated
4GG	19.4	721.21334	$C_{37}H_{37}O_{15}$	−0.6	T-(4-O-β)-G-(4-O-β)-G	Annotated
4GG	19.6	721.21185	$C_{37}H_{37}O_{15}$	−2.7	T-(4-O-β)-G-(4-O-β)-G	Characterized
4GG	19.8	721.21251	$C_{37}H_{37}O_{15}$	−1.8	T-(4-O-β)-G-(4-O-β)-G	Annotated
4GG	20.0	721.21093	$C_{37}H_{37}O_{15}$	−4	T-(4-O-β)-G-(4-O-β)-G	Annotated
4sG	19.8	751.22302	$C_{38}H_{39}O_{16}$	−1.8	T-(4-O-βt)-S-(4-O-βt)-G	Identified
4sG	20.3	751.22338	$C_{38}H_{39}O_{16}$	−1.3	T-(4-O-βe)-S-(4-O-βt)-G	Identified
4sG	20.6	751.22316	$C_{38}H_{39}O_{16}$	−1.6	T-(4-O-β)-S-(4-O-β)-G	Characterized
4sG	21.0	751.22285	$C_{38}H_{39}O_{16}$	−2	T-(4-O-β)-S-(4-O-β)-G	Characterized
4GG'	22.7	763.22264	$C_{39}H_{39}O_{16}$	−2.3	T-(4-O-β)-G-(4-O-β)-G'	Annotated
4G'G	23.2	763.22198	$C_{39}H_{39}O_{16}$	−3.1	T-(4-O-β)-G'-(4-O-β)-G	Annotated
4G'G	23.5	763.22264	$C_{39}H_{39}O_{16}$	−2.2	T-(4-O-β)-G'-(4-O-β)-G	Annotated
4G'G	24.0	763.22147	$C_{39}H_{39}O_{16}$	−3.8	T-(4-O-β)-G'-(4-O-β)-G	Annotated
5Gs''	24.3	879.24808	$C_{47}H_{43}O_{17}$	−2.8	T-(4-O-β)-G-(5-β)-S''	Characterized/annotated
5Gs'' [**5G''s**]	25.2	879.24942	$C_{47}H_{43}O_{17}$	−1.3	T-(4-O-β)-G-(5-β)-S'' [T-(4-O-β)-G''-(5-β)-S]	Characterized
5Gs''	25.7	879.24975	$C_{47}H_{43}O_{17}$	−0.9	T-(4-O-β)-G-(5-β)-S''	Characterized/annotated
5Gs'' [**5G''s**]	26.3	879.24928	$C_{47}H_{43}O_{17}$	−1.5	T-(4-O-β)-G-(5-β)-S'' [T-(4-O-β)-G''-(5-β)-S]	Characterized
5Gs'' [**5G''s**]	26.9	879.24915	$C_{47}H_{43}O_{17}$	−1.6	T-(4-O-β)-G-(5-β)-S'' [T-(4-O-β)-G''-(5-β)-S]	Characterized
5Gs'' [**5G''s**]	27.4	879.24823	$C_{47}H_{43}O_{17}$	−2.7	T-(4-O-β)-G-(5-β)-S'' [T-(4-O-β)-G''-(5-β)-S]	Characterized
4G''G [**4GG''**]	24.8	867.24907	$C_{46}H_{43}O_{17}$	−1.7	T-(4-O-β)-G''-(4-O-β)-G [T-(4-O-β)-G-(4-O-β)-G'']	Characterized
4G''G [**4GG''**]	25.0	867.24993	$C_{46}H_{43}O_{17}$	−0.7	T-(4-O-β)-G''-(4-O-β)-G [T-(4-O-β)-G-(4-O-β)-G'']	Characterized
4G''G [**4GG''**]	25.7	867.24982	$C_{46}H_{43}O_{17}$	−0.9	T-(4-O-β)-G''-(4-O-β)-G [T-(4-O-β)-G-(4-O-β)-G'']	Annotated
4GG''	26.0	867.24835	$C_{46}H_{43}O_{17}$	−2.6	T-(4-O-β)-G-(4-O-β)-G''	Annotated
4G''G [**4GG''**]	26.3	867.24938	$C_{46}H_{43}O_{17}$	−1.4	T-(4-O-β)-G''-(4-O-β)-G/ T-(4-O-β)-G-(4-O-β)-G''	Characterized
4G''G [**4GG''**]	26.5	867.24895	$C_{46}H_{43}O_{17}$	−1.9	T-(4-O-β)-G''-(4-O-β)-G/ T-(4-O-β)-G-(4-O-β)-G''	Characterized
4Gs''	26.2	897.25787	$C_{47}H_{45}O_{18}$	−3.6	T-(4-O-β)-G-(4-O-β)-S''	Annotated
4Gs''	26.4	897.25903	$C_{47}H_{45}O_{18}$	−2.3	T-(4-O-β)-G-(4-O-β)-S''	Annotated
4Gs''	26.5	897.25803	$C_{47}H_{45}O_{18}$	−3.5	T-(4-O-β)-G-(4-O-β)-S''	Annotated
4Gs''	26.7	897.25813	$C_{47}H_{45}O_{18}$	−3.4	T-(4-O-β)-G-(4-O-β)-S''	Annotated
4Gs''	26.9	897.25816	$C_{47}H_{45}O_{18}$	−3.3	T-(4-O-β)-G-(4-O-β)-S''	Annotated

[a]Identified indicates a structure confirmed by comparison with the synthesized authentic compound; annotated indicates a rather firm structural elucidation based on comparison of the MS^n spectrum with those of identified structural analogs and on the accurate m/z value; characterized indicates a fairly high degree of certainty in the structural elucidation that is based on the MS^n spectral interpretation, accurate m/z value, and data available from the literature and public databases. In shorthand names, *t* and *e* descriptors are for *threo* (= *syn*) and *erythro* (= *anti*) isomers. t_R = retention time.

tricin-containing metabolites extracted from maize. In addition, the synthetic compounds helped in verifying whether any compounds extracted from the maize internodes had escaped the CSPP network algorithm.

The syntheses of **3H**, **3G**, **3S**, and **4SG** were described in detail in a previous study (Lan et al., 2015). The products **3G′/S′** and **3G″/S″** (Fig. 2) of tricin's coupling with acetylated and *p*-coumaroylated monolignols were prepared by modifications to the syntheses of their parent compounds. The preparation begins with the coupling of bromo-ketones **7** to a suitably protected tricin derivative **6**, followed by retro-aldol addition of formaldehyde to create the lignin unit's three-carbon side chain, the synthesis of which has been described (Lan et al., 2015). At this point, the product is suitably protected but bears the free γ-OH to allow acylation with *p*-coumarate or acetate to provide the acylated precursors **11** and **12**. Deprotection of phenolic acetyl and methoxymethyl groups and reduction of the benzylic ketone then affords the

required conjugates **3G′/S′** and **3G″/S″**. Full synthetic details, along with the NMR characterization, are provided in Supplemental Data S1.

Metabolite Authentication and Isomer Analysis

The eight synthetic compounds were used to authenticate the maize metabolites, and six of them could be identified in the methanol extracts from maize. Interestingly, whereas the trimer **4SG** could be authenticated, its parent compound **3S**, along with the analog **3S′** from sinapyl acetate, were below the detection limit in the maize extract (Figs. 3 and 4). In addition, tricin coupled with the sinapyl *p*-coumarate conjugate, dimer **3S″**, could be authenticated. These observations presumably reflect the relative coupling propensities of the various dimers, suggesting that coniferyl alcohol, for example, may couple faster with dimer **3S** than with the *p*-coumaroylated dimer **3S″**.
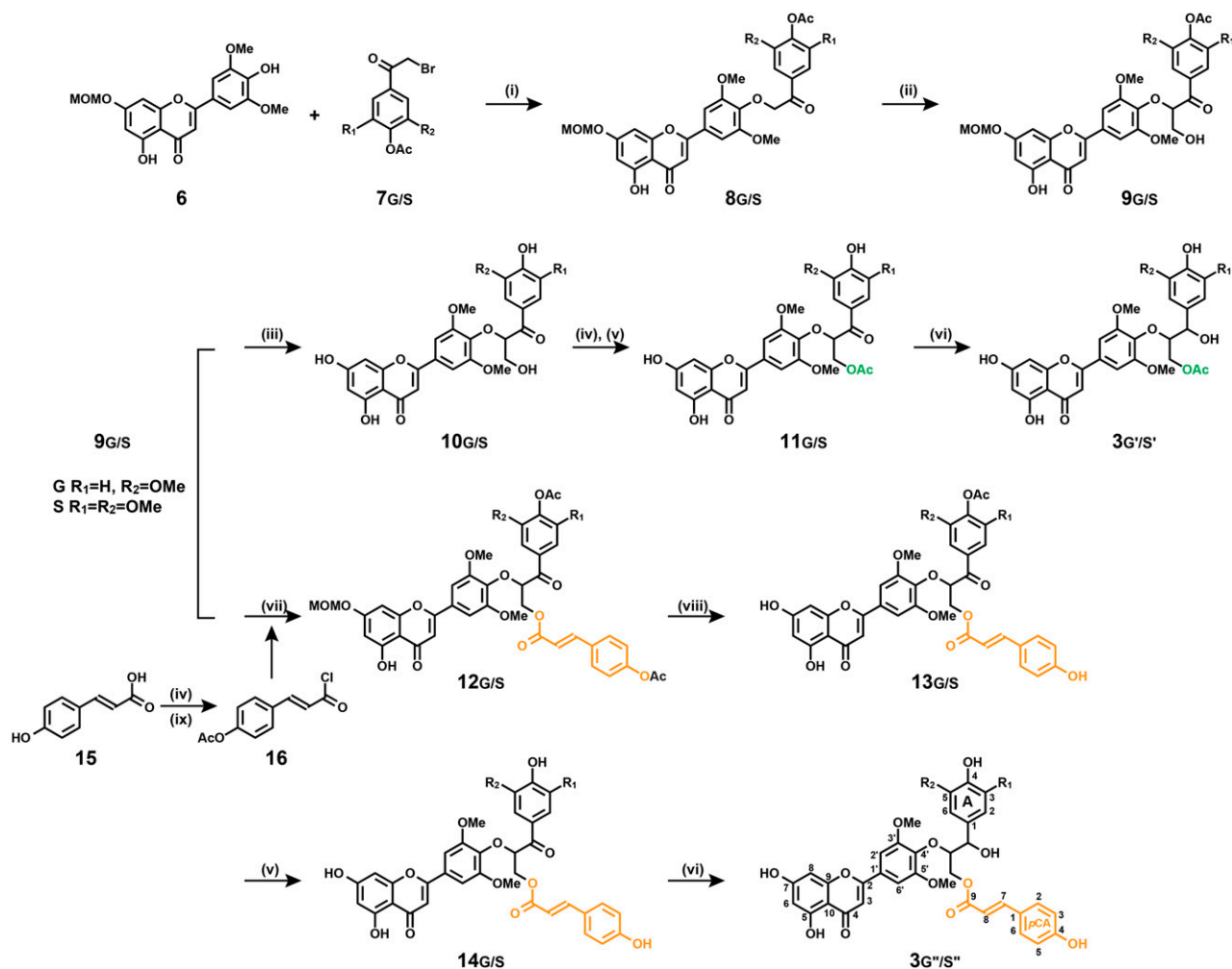
Figure 2. Synthesis of tricin-monolignol, tricin-monolignol acetate, and tricin-monolignol *p*-coumarate dimeric products **3G′/S′** and **3G″/S″**: (i) K$_2$CO$_3$, *N*,*N*-dimethylformamide; (ii) formaldehyde, K$_2$CO$_3$, dioxane; (iii) methanol/CHCl$_3$, HCl; (iv) pyridine/acetic anhydride; (v) ammonium acetate, methanol; (vi) borane-*tert*-butylamine complex, CH$_2$Cl$_2$; (vii) acetylated *p*-coumaroyl chloride, 4-dimethylaminopyridine (DMAP), CH$_2$Cl$_2$; (viii) ethylene glycol, 120°C; and (ix) toluene, thionyl chloride.

We examined the distribution of diastereomers of the tricin-containing dimers and their acetate and *p*-coumarate derivatives (Fig. 3) for both the synthetic products and their counterparts in maize metabolites. Such dimeric compounds were each separable as two peaks in an HPLC scan, which represent *syn* and *anti* isomers, indicated by comparing the retention times of authentic compounds and the MS² spectra from the two peaks (Fig. 3). In addition, as can be seen from Figure 4, most of the trimeric compounds revealed more than four (usually more than six) peaks, and it is reasonable to conclude that the larger peaks are from two overlapping isomers. Therefore, it is evident that such spectra from compounds **4** result from the eight possible isomers in each case; there are four optical centers affording 2^4 optical isomers and half that number ($2^3 = 8$) of physically distinct isomers. The β-5 trimer labeled **5GS″** in Figure 4 should have only four isomers, so the

observation of at least six distinct peaks, two of which are again larger and likely from two overlapping isomers, suggests that both regioisomers (**5GS″** and **5G″S**) appear in the same area of the chromatogram here (Table I). We further examined the enantiomers of the tricin-oligolignol dimers from maize, using **3H** and **3G** as examples, using an LC-MS device equipped with a chiral column and the multiple reaction monitoring (MRM) mass spectrometric technique. The MRM mode has the advantage of selectivity and improved quantitation for trace amounts of compounds. The chiral chromatogram (Fig. 5) shows three peaks, one of which corresponds to the *syn* isomers (with two enantiomers overlapping) and the other two with similar peak areas originating from the *anti* isomers (two separated enantiomers), indicating that both the *syn* and *anti* isomers are racemic, just like their synthesized analogs.
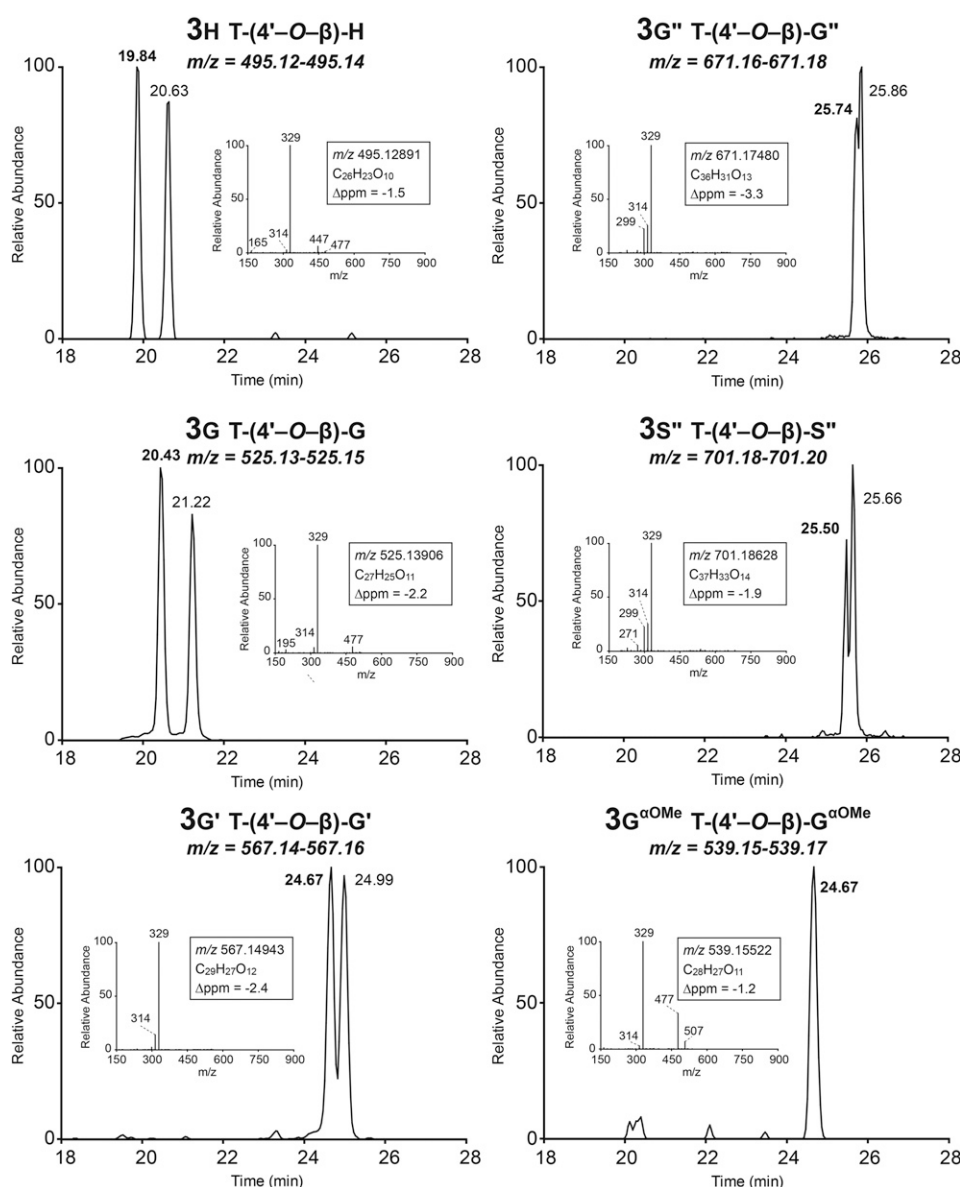
Figure 3. LC-MS of monolignol and acylated monolignol coupling products with tricin (dimers 3).

Figure 4. LC-MS of trimeric compounds **4** and **5** formed between tricin and various monolignols and acylated monolignols.
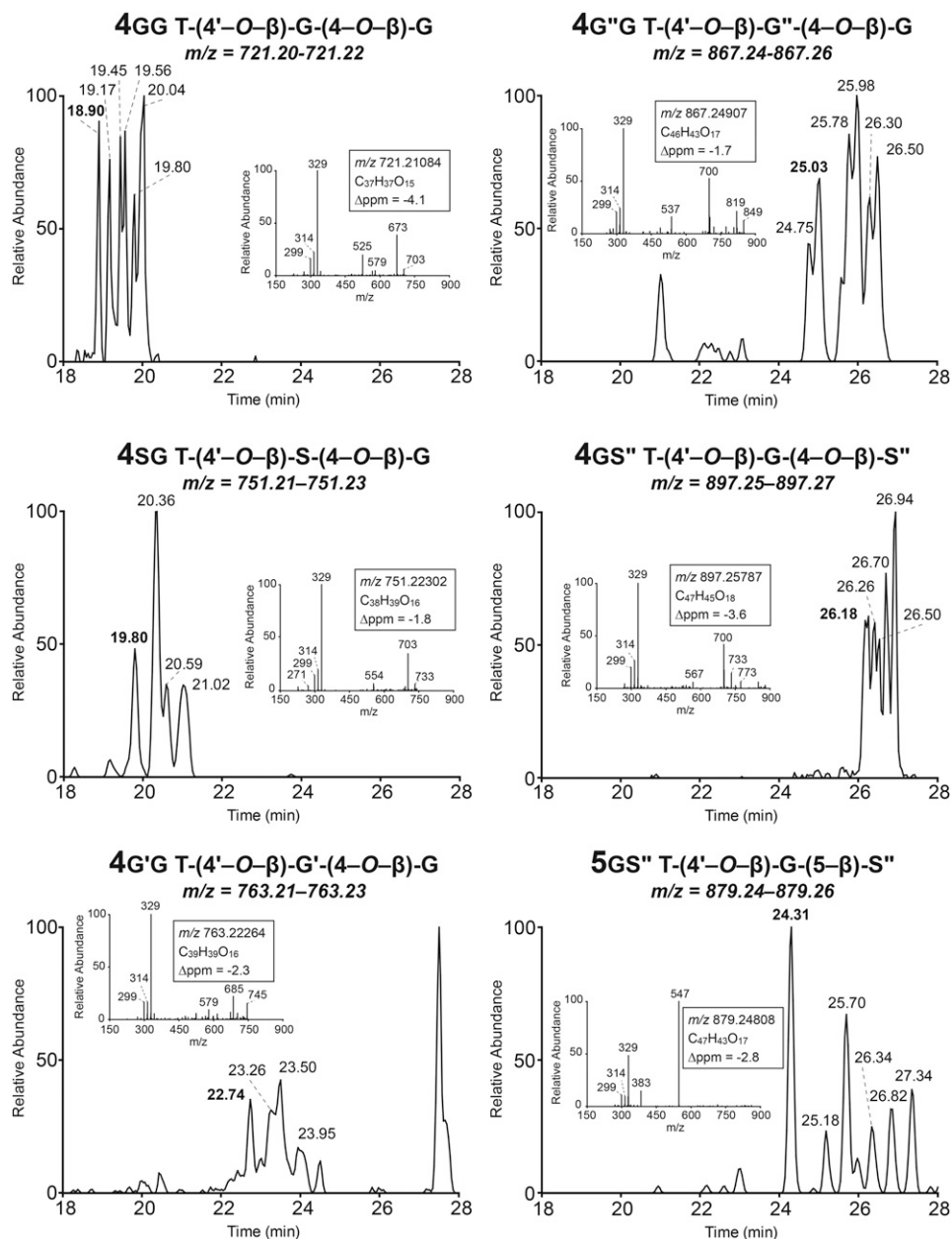
DISCUSSION

Tricin Couples with Monolignol Acetate and *p*-Coumarate Conjugates

One of the most interesting findings from this maize metabolite profiling is not just the presence of tricin-oligolignols but also of their acetate and *p*-coumarate analogs (Figs. 1, 3, and 4). *p*-Coumarate has long been a known feature of monocot lignins, where it is found acylating the γ-OH of lignin side chains (Ralph et al., 1994; Grabber et al., 1996; Ralph, 2010). Such acylation has now been compellingly demonstrated to arise via lignification with biosynthesized monolignol conjugates **2″** (Lu and Ralph, 2008; Ralph, 2010; Lan et al., 2015; Lu et al., 2015). The monolignol:*p*-coumaroyl-coenzyme A transferase

(PMT) enzyme and the *PMT* gene involved have been identified and the function proven via knockout, down-regulation, and overexpression (Withers et al., 2012; Marita et al., 2014; Petrik et al., 2014). Acetates are also well known to acylate monolignols in various plant lines (Ralph, 1996; del Río et al., 2007, 2008, 2012a, 2012b; Lu and Ralph, 2008; Martínez et al., 2008; Rencoret et al., 2013), although the responsible transferase protein and the corresponding gene have not been unambiguously identified to date. Monocots have more extensive lignin acetylation than was realized previously (del Río et al., 2007, 2008, 2012a, 2012b, 2015; Martínez et al., 2008; Rencoret et al., 2013). The products **3G′** from tricin's cross coupling with acetylated monolignols **2′** here (Fig. 1) further confirm the
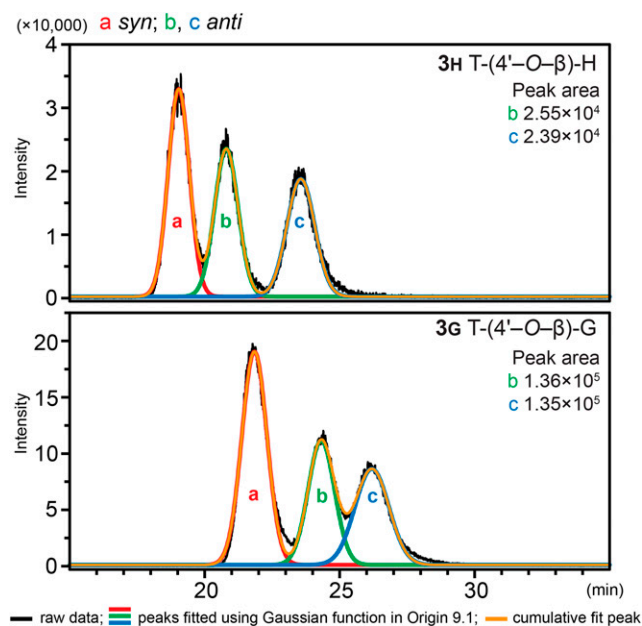
Figure 5. Chiral chromatography of **3H** and **3G** in maize extracts, by LC-MS using MRM detection, showing their racemic nature.

involvement of monolignol acetate conjugates in maize (and other monocot) lignification.

Structural Analyses of Tricin-Oligolignols Support the Combinatorial Radical Coupling Theory

The above finding that monolignols **2** as well as their acetate and *p*-coumarate conjugates **2′** and **2″** all couple with tricin (Figs. 3 and 4) has deeper consequences regarding lignification. As in the established theory (Harkin, 1967; Freudenberg and Neish, 1968) and as increasingly evidenced (Ralph et al., 2004b, 2008; Vanholme et al., 2010), lignins are the products of simple, but combinatorial, radical coupling chemistry. They are consequently racemic polymers, are characterized by being products with a huge number of possible isomers, and have no defined sequence or (repeating) structure, a position that was heatedly debated after notions of absolute proteinaceous control over lignin structure were championed for a period (Davin and Lewis, 2005). Such impressions continue to be eroded as evidence accumulates from various structural studies of natural plants along with the rich variety of monolignol biosynthetic pathway mutants and transgenics, reestablishing the validity of the original theory (Ralph et al., 2008). The results here further add to the evidence.

Another key argument supporting the combinatorial coupling theory follows from the separation and identification of the enantiomers of **3G** and **3H**. Compound **3G** was isolated previously from *Avena sativa* by capillary electrophoresis; as both of the diastereomers were enantiomerically pure, they were termed flavonolignans (Wenzig et al., 2005). In our study, however, the two

enantiomers of *anti* **3G** and *anti* **3H** isolated from maize were successfully separated using chiral-column HPLC, as confirmed by MRM on mass spectrometry that is able to accurately track compounds at low levels; the similar peak areas (Fig. 5) indicate the racemic nature of both, as has been reported for various lignin units (Ralph et al., 1999; Akiyama et al., 2015). Importantly, therefore, these dimeric compounds **3**, resulting from the coupling of tricin and a monolignol, cannot be termed flavonolignans (which, like their component lignan moieties [Umezawa, 2004], would logically be optically active); therefore, they should be considered to be oligomers that are destined for the fully racemic lignins and are suggested to be generally termed flavonolignin oligomers or, specifically, tricin-oligolignols. Optical activity determinations are not always carried out, so it is not always possible to determine whether the extracted components are (optically active) lignans or (racemic) dilignols and oligolignols, as discussed briefly previously (Dima et al., 2015); the same is true here for these flavonolignans versus flavonolignols.

The variety of tricin-oligolignols and their variously acylated counterparts, and the identification of their diastereomers and enantiomers, provide compelling new evidence for the combinatorial nature of lignification: available monomer radicals, including those from tricin and the monolignol conjugates, will couple and cross couple subject only to their chemical propensities for doing so. Therefore, we observe certain combinatorial possibilities for the cross coupling of both coniferyl and sinapyl acetates and *p*-coumarates, along with the parent monolignols, with tricin, as shown schematically in Figure 1. The trimers and tetramers then attest to the chain extension via further coupling from among the available monolignols and their conjugates. Importantly, the products observed here also provide evidence for the growth of the polymer in the endwise coupling sense (Freudenberg, 1956; Ralph et al., 2004b), in which chain extension is via monomer addition to the phenolic end of the growing oligomer, and are not consistent with the notion of the tricin-containing polymeric units being derived from preformed flavonolignans. All that perhaps remains surprising is that all of these monomeric entities must be present at the same time and space, an observation that might not have been expected; in dicots, for example, sinapyl alcohol enters lignification later in cell wall development, preceded by *p*-coumaryl alcohol and then coniferyl alcohol, although there is overlap (Terashima et al., 1993). Essentially nothing is known about the temporal (or spatial) nature of monolignol conjugate incorporation into monocot lignins.

Finally, again given that tricin can only start a chain, and given that it is present at significant levels (currently estimated to be 1.5% of the lignin in the wild-type maize internode samples analyzed here, according to the thioacidolysis method; W.L., J.Ra, unpublished data), it must nucleate a fraction of the lignin chains. The identification of compound **3H**, the coupling product of tricin with *p*-coumaryl alcohol, suggests that tricin is present early in lignification. Tricin is noted to

be higher in concentration in younger and less lignified tissues (del Río et al., 2015), but it is not yet clear if it is biosynthesized throughout wall development. These revelations regarding tricin in lignins contributed to the resolution of a monocot-lignin structural dilemma that has existed for decades: that monocot lignins, unlike other syringyl-guaiacyl lignins in dicots/hardwoods, have essentially no, or very low levels of, resinols, syringaresinol, and pinoresinol (Marita et al., 2003; Lan et al., 2015). Such β-β-linked units are produced only as the result of monolignol (sinapyl alcohol) dimerization and are the obvious mechanism for starting a lignin chain. Maize whole cell wall or lignin NMR spectra had little evidence until recently of anything but β-ether units, with only a paucity of the other units (resinol [β-β], phenylcoumaran [β-5], dibenzodioxocin [5-5/4-O-β], and spirodienone [β-1]) seen in dicot lignins with a comparable syringyl-guaiacyl distribution (Lan et al., 2015). However, we recently disclosed the preponderance of sinapyl p-coumarate homodimerization units in maize lignins (Lan et al., 2015). Although this product is from β-β coupling, the γ-acylation does not allow resinol formation (Ralph, 2010), so its presence had been missed. Also, when the lignin chain is nucleated by another unit, such as tricin here (and as assumed for ferulate previously [Ralph et al., 1995], and in addition to it), lignification does not need to start with a dimerization reaction. The near absence of such resinol units in maize and some other monocots is now recognized as being a consequence of the nucleation of lignin chains by tricin and ferulate as well as from the surprising prevalence of acylated monolignol dimerization events in such lignins. Such features of the previously puzzling spectra of monocot lignins are now consistent with the evolving paradigms for the unique nature of lignification in monocots.

CONCLUSION

Following an analysis of maize metabolites by ultra-HPLC mass spectrometry, we have identified and characterized 12 tricin-oligolignols (Fig. 1) in some 42 resolved peaks (Table I) that include various diastereomers, the structures of which were further supported by comparison with independently synthesized authentic compounds. The maize metabolites include the 4'-O-β cross-coupling products between tricin and monolignols as well as their acetate and p-coumarate conjugates. Chiral chromatography of tricin-(4'-O-β)-p-coumaryl alcohol and tricin-(4'-O-β)-coniferyl alcohol coupling products from maize showed that the flavonolignols are fully racemic. The above findings provide compelling new evidence (1) for the natural cross coupling of tricin with monolignols and monolignol conjugates into flavonolignol dimers in planta; (2) that such dimers undergo further endwise coupling with additional monomers to form oligomers that are destined for lignin polymers in which chains are started by tricin; and (3) for the combinatorial nature of lignification (i.e. supporting the theory that lignin polymers are formed by combinatorial radical coupling chemistry independent of proteinaceous control).

MATERIALS AND METHODS

General

All chemicals and solvents used in this study were from commercial sources and used without further purification. Preparative thin-layer chromatography (TLC) plates (1 or 2 mm thickness, 20 cm × 20 cm, normal phase) were purchased from Analtech. Flash chromatography was conducted on an Isolera One instrument (Biotage) with Biotage snap silica cartridges. The eluent for chromatography was hexane/ethyl acetate or methanol/dichloromethane as described. NMR spectra were recorded at 25°C on a Bruker Biospin AVANCE 500- or 700-MHz spectrometer fitted with a cryogenically cooled 5-mm ^{1}H/^{13}C-optimized triple resonance (^{1}H/^{13}C/^{15}N, TCI, 500 MHz) or ^{1}H-optimized triple resonance (^{1}H/^{13}C/^{15}N, TXI, 700 MHz) gradient probe with inverse geometry (proton coil closest to the sample). Bruker's Topspin 3.1 (Mac) software was used to process the spectra. The central solvent peak was used as an internal reference (δ_C/δ_H: acetone-d_6, 29.84/2.04). The standard Bruker implementations of one-dimensional and two-dimensional (gradient-selected correlation spectroscopy, heteronuclear single-quantum coherence, and heteronuclear multiple-bond correlation) NMR experiments were used for routine structural assignments of newly synthesized compounds.

Syntheses of Arylglycerol-β-O-4'-Tricin Ethers 3 and 4

Compounds 3H, 3G, 3s, and 4sG were synthesized as described recently (Lan et al., 2015).

Syntheses of γ-Acylated Arylglycerol-β-O-4'-Tricin Ethers 3' and 3''

Figure 2 outlines the synthetic procedure for both the normal and γ-acylated arylglycerol-β-O-4'-tricin ethers 3' and 3''; details are provided below. Compounds 6, 7G/s, 8G/s, 9G/s, and 10G/s were synthesized according to the methods described previously (Lan et al., 2015).

Compound 11G/S

Compound 10G (50 mg, 95.3 μmol) was first acetylated in pyridine:acetic anhydride (2:1, v/v; 5 mL) at room temperature for 2 h. The solution was extracted with ethyl acetate (25 mL) and acidic water (pH 2; 25 mL). Ethyl acetate layers were combined and washed with saturated ammonium chloride solution (50 mL) and dried over anhydrous magnesium sulfate. After condensation, the acetylated product and ammonium acetate (146.9 mg, 1.9 mmol) were added to methanol (20 mL) and heated at 50°C to remove the phenolic acetate group. When the starting material had totally disappeared (approximately 8 h, monitored by TLC), the solvent was evaporated under reduced pressure and the resulting material was subjected to TLC purification to give 11G (82% yield). 11s was synthesized analogously in 80% yield.

Compound 3G'/S'

Borane-tert-butylamine complex (19.2 mg, 220.6 μmol) and 11G (25 mg, 44.1 μmol) were dissolved in CH$_2$Cl$_2$ (5 mL) at room temperature. The solvent was removed under reduced pressure after the reaction was completed (approximately 12 h, monitored by TLC). The product was dissolved in ethyl acetate: water (10:1, v/v; 25 mL) with 1 mL of 6 M HCl solution and stirred for 1 h to break down the borate intermediates. The mixture solution was washed with water and saturated ammonium chloride solution (50 mL). The ethyl acetate layer was separated, dried over anhydrous magnesium sulfate, and filtered, and the solvent was removed under reduced pressure to produce 3G' (92%). 3s' was prepared analogously in 90% yield.

Compound 12G/S

Acylation of 9G/s was catalyzed by DMAP in CH$_2$Cl$_2$. A detailed procedure is given using 12G as an example. 9G (250 mg, 409.4 μmol) was dissolved in CH$_2$Cl$_2$ (10 mL), to which freshly made acetylated p-coumaroyl chloride 16 (110 mg, 490.5 μmol) and DMAP (50 mg, 409.3 μmol) were added. After 1 h, the

solution was washed with 0.5 M HCl solvent (3 × 50 mL) to remove DMAP. The CH₂Cl₂ solution was dried over anhydrous magnesium sulfate and filtered, and the solvent was removed under reduced pressure. TLC purification using CH₂Cl₂ and methanol (40:1, v/v) as eluent was conducted, giving 67%/84% yield of **12G/S**.

Compound 13G/S

Selective deprotection of the methoxylmethyl group was achieved in ethylene glycol as described previously (Miyake et al., 2004). **12G/S** (100 mg, 125.2 μmol for guaiacyl, 120.7 μmol for syringyl) was mixed with ethylene glycol (25 mL) and heated at 120°C for 3 h. Then, water (25 mL) was added to quench the reaction. Ethyl acetate (3 × 25 mL) was used to extract the products. The combined ethyl acetate fraction was dried over anhydrous magnesium sulfate and filtered, and the solvent was evaporated under reduced pressure. TLC purification using CH₂Cl₂ and methanol (40:1, v/v) as eluent yielded **13G/S** (43%/56%).

Compound 14G/S

The phenolic acetate group of **13G/S** was eliminated using ammonium acetate in methanol as described for the synthesis of **11G/S**. The yield of **14G/S** was 64%/71%.

Compound 3G′′/S′′

Borane-*tert*-butylamine complex was used to reduce the α-ketone in **13G/S** to its alcohol, as above for the synthesis of **3G′/S′**. The yield of **3G′′/S′′** was 80%/75%.

Compound 16

p-Coumaric acid **15** (1 g, 4.8 mmol) was first acetylated in pyridine:acetic anhydride (2:1, v/v; 15 mL). The acetylated product and thionyl chloride (1 mL, 13.8 mmol) were added to toluene (10 mL) and heated, with stirring, to 100°C until the material was completely dissolved (approximately 1 h). Then, the solvent was evaporated under reduced pressure. The product was dissolved in toluene (50 mL) and evaporated again. This procedure was repeated several times to eliminate residual thionyl chloride. The final acyl chloride product **16** was obtained as a white powder in 96% yield.

Growth Conditions and Extraction

Maize (*Zea mays*) plants (inbred line B104) were grown in a greenhouse (16 h of light; minimum temperature of 25°C and 23°C during the day and night, respectively). Supplementary light was added using high-pressure sodium vapor lamps when natural light intensity dropped below 200 W m⁻². Fertilizer was added with the water supply (Ec = 1 mS cm⁻¹, NPK = 20:5:20, MgO = 3). The ninth internode (the internode just below the cob) was dissected from 22 plants harvested 7 d after silking. At this time, the plants had reached a height of 2 m. Internode samples were ground using liquid nitrogen-cooled Retch Grinding Jars MM 400 Stainless Steel 50 mL. A volume of 500 μL of powder was extracted with 1 mL of methanol at 70°C for 15 min. Following evaporation, the pellet was dissolved in 300 μL of MilliQ water:cyclohexane (2:1, v/v). Ten microliters of the aqueous phase was used for metabolite profiling.

Metabolite Profiling

Reverse-phase ultra-HPLC coupled to Fourier transform-ion cyclotron resonance-mass spectrometry was performed on a previously described platform (Accela coupled to a LTQ FT Ultra device; Thermo Electron) using the conditions described previously (Morreel et al., 2014) with some modifications. The applied gradient was as follows: 0 min, 95% A; 30 min, 55% A; and 35 min, 0% A (solvents A and B were aqueous 0.1% acetic acid and acetonitrile:water [99:1, v/v], respectively). Electrospray ionization source conditions were as follows: spray voltage, 3.5 kV; sheath gas, 10 (arbitrary); and auxiliary gas, 15 (arbitrary). Full Fourier transform mass spectra were recorded between 120 and 1,200 *m/z*. Data-dependent MS² spectra of the four most abundant ions in the previous full mass spectra were recorded using the ion-trap analyzer. Integration, alignment, grouping of *m/z* features derived from the same compound, and generation of the CSPP network were performed as described previously (Morreel et al., 2014). Structural characterization of the tricin-oligolignols was further aided via MSⁿ-based oligolignol sequencing (Morreel et al., 2010a,

2010b). The latter method unveiled some typical characteristics in the gas-phase fragmentation of tricin-oligolignols. A full analysis of the CSPP network characteristics of these and other monocot-specific compounds will be published elsewhere.

MS² Analysis of Tricin-Oligolignols 3 and 4

Upon CID, 4′-O-β-type oligolignols undergo characteristic gas-phase fragmentation channels involving the 7-OH function (Morreel et al., 2010a, 2010b). One series of fragmentations (called type I fragmentations) yield small neutral losses, of which the 48-D loss often leads to the base peak in the CID spectrum, especially in the case of a *threo* configuration of the 4′-O-β-linkage (Morreel et al., 2004a). The 48-D loss results from expelling the 7- and 9-OH groups as water and formaldehyde, respectively (Morreel et al., 2010a). Type II fragmentations lead to the cleavage of the 4′-O-β-linkage and allow characterization of the units connected by it (Morreel et al., 2010a). The precursor ions of all 4′-O-β-coupled tricin-type oligolignols are subjected to type I and II gas-phase fragmentations similar to those described for traditional oligolignols. Nevertheless, their MS² spectra were quite often dominated by a tricin product ion (*m/z* 329) resulting from a type II fragmentation. Clearly, this fragmentation channel is favored, as the charge of the ion can be readily delocalized across the extensive conjugated π system.

Chiral Chromatography of Synthetic Dimers and Their Maize-Derived Counterparts

Separation of the enantiomers of **3H** and **3G** (for both synthetic compounds and methanol extracts from maize) was accomplished on an LC-MS system (Shimadzu) equipped with two LC-20AD pumps, a SIL-20AC HT autosampler, a CTO-20A column oven, a CBM-20A controller, and an LCMS-8040 triple-quadrupole mass spectrometer using a Lux Cellulose-1 (150 × 4.6 mm, 5 μm; Phenomenex) column at 40°C. A dual ion source method was applied for ionization. The mobile phase was water (solvent A) and methanol (solvent B) with 0.1% (v/v) formic acid in each solution, and 60% of solvent B was used as an eluent. The injection volume was 1 μL, and the flow rate was 0.7 mL min⁻¹. Detection was achieved using MRM mode, in which the first quadrupole was conducted in single-ion monitoring mode for a set *m/z* value, and the target ion (precursor) becomes broken down into fragments (products) using an optimal collision energy before entering the second quadrupole region, followed by single-ion monitoring in the third quadrupole to track the fragments. The chiral chromatogram was analyzed in Origin 9.1 for multiple peak fitting using a Gaussian function.

Supplemental Data

The following supplemental materials are available.

Supplemental Figure S1. LC-MS trace and the MS² spectra of each peak for **4GG** and **4SG**.

Supplemental Data S1. ¹H and ¹³C NMR data for synthetic compounds.

LITERATURE CITED

Akiyama T, Magara K, Meshitsuka G, Lundquist K, Matsumoto Y (2015) Absolute configuration of β- and α-asymmetric carbons within β-O-4-structures in hardwood lignin. J Wood Chem Technol **35:** 8–16

Boerjan W, Ralph J, Baucher M (2003) Lignin biosynthesis. Annu Rev Plant Biol **54:** 519–546

Bonawitz ND, Chapple C (2010) The genetics of lignin biosynthesis: connecting genotype to phenotype. Annu Rev Genet **44:** 337–363

Bouaziz M, Veitch NC, Grayer RJ, Simmonds MSJ, Damak M (2002) Flavonolignans from *Hyparrhenia hirta*. Phytochemistry **60:** 515–520

Davin LB, Lewis NG (2005) Lignin primary structures and dirigent sites. Curr Opin Biotechnol **16:** 407–415

del Río JC, Lino AG, Colodette JL, Lima CF, Gutiérrez A, Martínez AT, Lu F, Ralph J, Rencoret J (2015) Differences in the chemical structure of the lignins from sugarcane bagasse and straw. Biomass Bioenergy **81:** 322–328

del Río JC, Marques G, Rencoret J, Martínez AT, Gutiérrez A (2007) Occurrence of naturally acetylated lignin units. J Agric Food Chem **55:** 5461–5468

del Río JC, Prinsen P, Rencoret J, Nieto L, Jiménez-Barbero J, Ralph J, Martínez ÁT, Gutiérrez A (2012a) Structural characterization of the lignin in the cortex and pith of elephant grass (*Pennisetum purpureum*) stems. J Agric Food Chem **60:** 3619–3634

del Río JC, Rencoret J, Marques G, Gutiérrez A, Ibarra D, Santos JI, Jiménez-Barbero J, Zhang L, Martínez AT (2008) Highly acylated (acetylated and/or *p*-coumaroylated) native lignins from diverse herbaceous plants. J Agric Food Chem **56:** 9525–9534

del Río JC, Rencoret J, Prinsen P, Martínez ÁT, Ralph J, Gutiérrez A (2012b) Structural characterization of wheat straw lignin as revealed by analytical pyrolysis, 2D-NMR, and reductive cleavage methods. J Agric Food Chem **60:** 5922–5935

Dima O, Morreel K, Vanholme B, Kim H, Ralph J, Boerjan W (2015) Small glycosylated lignin oligomers are stored in *Arabidopsis* leaf vacuoles. Plant Cell **27:** 695–710

Dixon RA, Reddy MS (2003) Biosynthesis of monolignols: genomic and reverse genetic approaches. Phytochem Rev **2:** 289–306

Freudenberg K (1956) Beiträge zur Erforschung des Lignins. Angew Chem **68:** 508–512

Freudenberg K, Neish AC (1968) Constitution and Biosynthesis of Lignin. Springer-Verlag, Berlin

Grabber JH, Quideau S, Ralph J (1996) *p*-Coumaroylated syringyl units in maize lignin: implications for *β*-ether cleavage by thioacidolysis. Phytochemistry **43:** 1189–1194

Harkin JM (1967) Lignin: a natural polymeric product of phenol oxidation. *In* WI Taylor, AR Battersby, eds, Oxidative Coupling of Phenols. Marcel Dekker, New York, pp 243–321

Lan W, Lu F, Regner M, Zhu Y, Rencoret J, Ralph SA, Zakai UI, Morreel K, Boerjan W, Ralph J (2015) Tricin, a flavonoid monomer in monocot lignification. Plant Physiol **167:** 1284–1295

Li M, Pu Y, Yoo CG, Ragauskas AJ (2016) The occurrence of tricin and its derivatives in plants. Green Chem **18:** 1439–1454

Lu F, Karlen SD, Regner M, Kim H, Ralph SA, Sun R, Kuroda K, Augustin MA, Mawson R, Sabarez H, et al (2015) Naturally *p*-hydroxybenzoylated lignins in palms. BioEnergy Res **8:** 934–952

Lu F, Ralph J (2008) Novel tetrahydrofuran structures derived from *β-β*-coupling reactions involving sinapyl acetate in Kenaf lignins. Org Biomol Chem **6:** 3681–3694

Marita JM, Hatfield RD, Rancour DM, Frost KE (2014) Identification and suppression of the *p*-coumaroyl CoA:hydroxycinnamyl alcohol transferase in *Zea mays* L. Plant J **78:** 850–864

Marita JM, Vermerris W, Ralph J, Hatfield RD (2003) Variations in the cell wall composition of maize *brown midrib* mutants. J Agric Food Chem **51:** 1313–1321

Martínez AT, Rencoret J, Marques G, Gutiérrez A, Ibarra D, Jiménez-Barbero J, del Río JC (2008) Monolignol acylation and lignin structure in some nonwoody plants: a 2D NMR study. Phytochemistry **69:** 2831–2843

Miyake H, Tsumura T, Sasaki M (2004) Simple deprotection of acetal type protecting groups under neutral conditions. Tetrahedron Lett **45:** 7213–7215

Morreel K, Dima O, Kim H, Lu F, Niculaes C, Vanholme R, Dauwe R, Goeminne G, Inzé D, Messens E, et al (2010a) Mass spectrometry-based sequencing of lignin oligomers. Plant Physiol **153:** 1464–1478

Morreel K, Goeminne G, Storme V, Sterck L, Ralph J, Coppieters W, Breyne P, Steenackers M, Georges M, Messens E, et al (2006) Genetical metabolomics of flavonoid biosynthesis in *Populus*: a case study. Plant J **47:** 224–237

Morreel K, Kim H, Lu F, Dima O, Akiyama T, Vanholme R, Niculaes C, Goeminne G, Inzé D, Messens E, et al (2010b) Mass spectrometry-based fragmentation as an identification tool in lignomics. Anal Chem **82:** 8095–8105

Morreel K, Ralph J, Kim H, Lu F, Goeminne G, Ralph S, Messens E, Boerjan W (2004a) Profiling of oligolignols reveals monolignol coupling conditions in lignifying poplar xylem. Plant Physiol **136:** 3537–3549

Morreel K, Ralph J, Lu F, Goeminne G, Busson R, Herdewijn P, Goeman JL, Van der Eycken J, Boerjan W, Messens E (2004b) Phenolic profiling of caffeic acid *O*-methyltransferase-deficient poplar reveals novel benzodioxane oligolignols. Plant Physiol **136:** 4023–4036

Morreel K, Saeys Y, Dima O, Lu F, Van de Peer Y, Vanholme R, Ralph J, Vanholme B, Boerjan W (2014) Systematic structural characterization of metabolites in *Arabidopsis* via candidate substrate-product pair networks. Plant Cell **26:** 929–945

Mottiar Y, Vanholme R, Boerjan W, Ralph J, Mansfield SD (2016) Designer lignins: harnessing the plasticity of lignification. Curr Opin Biotechnol **37:** 190–200

Niculaes C, Morreel K, Kim H, Lu F, McKee LS, Ivens B, Haustraete J, Vanholme B, Rycke RD, Hertzberg M, et al (2014) Phenylcoumaran benzylic ether reductase prevents accumulation of compounds formed under oxidative conditions in poplar xylem. Plant Cell **26:** 3775–3791

Petrik DL, Karlen SD, Cass CL, Padmakshan D, Lu F, Liu S, Le Bris P, Antelme S, Santoro N, Wilkerson CG, et al (2014) *p*-Coumaroyl-CoA: monolignol transferase (PMT) acts specifically in the lignin biosynthetic pathway in *Brachypodium distachyon*. Plant J **77:** 713–726

Ralph J (1996) An unusual lignin from Kenaf. J Nat Prod **59:** 341–342

Ralph J (2010) Hydroxycinnamates in lignification. Phytochem Rev **9:** 65–83

Ralph J, Brunow G, Harris PJ, Dixon RA, Schatz PF, Boerjan W (2008) Lignification: are lignins biosynthesized via simple combinatorial chemistry or via proteinaceous control and template replication? *In* F Daayf, A El Hadrami, L Adam, GM Ballance, eds, Recent Advances in Polyphenol Research, Vol 1. Wiley-Blackwell Publishing, Oxford, UK, pp 36–66

Ralph J, Bunzel M, Marita JM, Hatfield RD, Lu F, Kim H, Schatz PF, Grabber JH, Steinhart H (2004a) Peroxidase-dependent cross-linking reactions of *p*-hydroxycinnamates in plant cell walls. Phytochem Rev **3:** 79–96

Ralph J, Grabber JH, Hatfield RD (1995) Lignin-ferulate crosslinks in grasses: active incorporation of ferulate polysaccharide esters into ryegrass lignins. Carbohydr Res **275:** 167–178

Ralph J, Hatfield RD, Quideau S, Helm RF, Grabber JH, Jung HJG (1994) Pathway of *p*-coumaric acid incorporation into maize lignin as revealed by NMR. J Am Chem Soc **116:** 9448–9456

Ralph J, Lundquist K, Brunow G, Lu F, Kim H, Schatz PF, Marita JM, Hatfield RD, Ralph SA, Christensen JH, et al (2004b) Lignins: natural polymers from oxidative coupling of 4-hydroxyphenylpropanoids. Phytochem Rev **3:** 29–60

Ralph J, Peng J, Lu F, Hatfield RD, Helm RF (1999) Are lignins optically active? J Agric Food Chem **47:** 2991–2996

Rencoret J, Ralph J, Marques G, Gutiérrez A, Martínez Á, del Río JC (2013) Structural characterization of lignin isolated from coconut (Cocos nucifera) coir fibers. J Agric Food Chem **61:** 2434–2445

Terashima N, Fukushima K, He LF, Takabe K (1993) Comprehensive model of the lignified plant cell wall. *In* HG Jung, DR Buxton, RD Hatfield, J Ralph, eds, Forage Cell Wall Structure and Digestibility. American Society of Agronomy/Crop Science Society of America/Soil Science Society of America, Madison, WI, pp 247–270

Umezawa T (2004) Diversity in lignan biosynthesis. Phytochem Rev **2:** 371–390

Vanholme R, Demedts B, Morreel K, Ralph J, Boerjan W (2010) Lignin biosynthesis and structure. Plant Physiol **153:** 895–905

Vanholme R, Morreel K, Ralph J, Boerjan W (2008) Lignin engineering. Curr Opin Plant Biol **11:** 278–285

Wenzig E, Kunert O, Ferreira D, Schmid M, Schühly W, Bauer R, Hiermann A (2005) Flavonolignans from *Avena sativa*. J Nat Prod **68:** 289–292

Withers S, Lu F, Kim H, Zhu Y, Ralph J, Wilkerson CG (2012) Identification of grass-specific enzyme that acylates monolignols with p-coumarate. J Biol Chem **287:** 8347–8355